SANDIA REPORT
SAND201X-XXXX
Unlimited Release
Printed Month and Year

Validation Assessment of a Glass-to-Metal Seal Finite-Element Model

Ryan D. Jamison, Thomas E. Buchheit, John M. Emery, Vicente J. Romero, Mark E. Stavig, Clay S. Newton, Arthur Brown

Prepared by
Sandia National Laboratories
Albuquerque, New Mexico 87185 and Livermore, California 94550

Sandia National Laboratories is a multimission laboratory managed and operated by National Technology and Engineering Solutions of Sandia, LLC, a wholly owned subsidiary of Honeywell International, Inc., for the U.S. Department of Energy's National Nuclear Security Administration under contract DE-NA0003525.

Issued by Sandia National Laboratories, operated for the United States Department of Energy by National Technology and Engineering Solutions of Sandia, LLC.

Available to DOE and DOE contractors from
U.S. Department of Energy
Office of Scientific and Technical Information
P.O. Box 62
Oak Ridge, TN 37831

Telephone: (865) 576-8401
Facsimile: (865) 576-5728
E-Mail: reports@osti.gov
Online ordering: http://www.osti.gov/scitech

Available to the public from
U.S. Department of Commerce
National Technical Information Service
5301 Shawnee Rd
Alexandria, VA 22312

Telephone: (800) 553-6847
Facsimile: (703) 605-6900
E-Mail: orders@ntis.gov
Online order: https://classic.ntis.gov/help/order-methods/

SAND201X-XXXX
Printed October 2017
Unlimited Release

Validation Assessment of a Glass-to-Metal Seal Finite-Element Model

Ryan D. Jamison
Transportation System Analysis

Thomas E. Buchheit
Component & Systems Analysis

John M. Emery
Solid Mechanics

Vicente J. Romero
V&V, UQ, Credibility Processes

Mark E. Stavig
Organic Materials Science

Clay S. Newton
Materials Mechanics and Tribology

Arthur Brown
Multi-Physics Modeling and Simulation

Sandia National Laboratories
P. O. Box 5800
Albuquerque, New Mexico 87185-MS0959

Abstract

Sealing glasses are ubiquitous in high pressure and temperature engineering applications, such as hermetic feed-through electrical connectors. A common connector technology are glass-to-metal seals where a metal shell compresses a sealing glass to create a hermetic seal. Though finite-element analysis has been used to understand and design glass-to-metal seals for many years, there has been little validation of these models. An indentation technique was employed to measure the residual stress on the surface of a simple glass-to-metal seal. Recently developed rate-dependent material models of both Schott 8061 and 304L VAR stainless steel have been applied to a finite-element model of the simple glass-to-metal seal. Model

predictions of residual stress based on the evolution of material models are shown. These model predictions are compared to measured data. Validity of the finite-element predictions is discussed. It will be shown that the finite-element model of the glass-to-metal seal accurately predicts the mean residual stress in the glass near the glass-to-metal interface and is valid for this quantity of interest.

ACKNOWLEDGMENTS

We would like to thank Jeff Payne and Diane Peebles for funding this work. Also, we'd like to recognize Robert Chambers, Dave Reedy, and Kevin Ewsuk for promoting the validation of a glass-to-metal seal model. Lastly, we'd like to thank our peer reviewers!

TABLE OF CONTENTS

1. Introduction 11

2. Experimental Results 12

   2.1. Room Temperature Creep 12

   2.2. Measuring Residual Stress 13

      2.2.1. Simple Concentric Seal 13

      2.2.2. Indentation Fracture Method Results 14

      2.2.3. Analysis of Residual Stress Results 16

3. Finite-Element model 18

   3.1. Model Description 18

   3.2. Schott 8061 Glass 18

   3.3. 304L VAR Stainless Steel 19

4. Model Comparison 21

   4.1. "Legacy" Material Models 22

   4.2. Rate-Dependent Material Models 23

   4.3. Modeling Assumption Uncertainty 25

   4.4. Model Validation Overview 28

5. Conclusions 30

6. References 31

FIGURES

Figure 1. Photo of Schott 8061 Bend Bar Subject to 3-Point Bend Dead Load at Room Temperature. 12

Figure 2. Measured Permanent Vertical Displacement in Solid Schott 8061 Glass. 13

Figure 3. Photo of the Concentric Glass-to-Metal Seal Used for Validation Purposes. 14

Figure 4. Measured Radial Stress in the Glass for Four Samples of the Concentric Seal Geometry. 15

Figure 5. Measured Hoop Stress in the Glass for Four Samples of the Concentric Seal Geometry. 16

Figure 6. Reduced Data Set of the Measured Radial Residual Stress. Solid Lines are the Mean and Dashed Lines are the 95/90 Tolerance Bounds. 17

Figure 7. Reduced Data Set of the Measured Hoop Residual Stress. Solid Lines are the Mean and Dashed Lines are the 95/90 Tolerance Bounds. 17

Figure 8. Cross-Section of the Concentric Seal Model Showing the Symmetry Planes. 18

Figure 9. Rate and Temperature Characterization Data and The Output from Model Calibration for 304L VAR Stainless Steel. 20

Figure 10. Residual Radial and Hoop Stress in the Glass of the GTMS at Room Temperature. ..22

Figure 11. Comparison Between Measured Radial Stress and Model Predictions with Thermoelastic Glass (TE) and Thermoelastic-Plastic Steel (MLTEP). 23

Figure 12. Comparison Between Measured Hoop Stress and Model Predictions with Thermoelastic Glass (TE) and Thermoelastic-Plastic Steel (MLTEP). 23

Figure 13. Comparison Between Measured Radial Stress and Model Predictions with Thermo-Viscoelastic Glass (SPEC) and Viscoplastic Steel (BCJ). 24

Figure 14. Comparison Between Measured Hoop Stress and Model Predictions with Thermo-Viscoelastic Glass (SPEC) and Viscoplastic Steel (BCJ). 25

Figure 15. Model Predictions of Residual Radial and Hoop Stress for Different Cooling Rates. 26

Figure 16. Model Predictions of Residual Radial and Hoop Stress for Perfectly Bonded and Constant Friction Material Interface. 27

Figure 17. Comparison Between Measured Radial Stress and Model Predictions After Aging and Polishing the GTMS. 28

Figure 18. Comparison Between Measured Hoop Stress and Model Predictions After Aging and Polishing the GTMS. 28

Figure 19. Model Predictions of Residual Radial and Hoop Stress Showing the Effect of Aging and Polishing. 29

TABLES

Table 1. Disposition of the Concentric Seal Samples Tested Using Indentation Fracture Method. 15

NOMENCLATURE

Abbreviation	Definition
BCJ	Bamman, Chiesa, and Johnson
°C	Degrees Celsius
CTE	Coefficient of thermal expansion
GTMS	Glass-to-metal seal
MLTEP	Multi-linear thermoelastic-plastic
r	Radial distance from the center of the concentric seal
SPEC	Simplified Potential Energy Clock Model
TE	Thermoelastic
VAR	Vacuum Arc Remelt

1. INTRODUCTION

Hermetic connectors are used in a variety of high-consequence applications such as the aerospace and medical communities. A common hermetic connector is a glass-to-metal seal (GTMS) which consists of a metal shell and glass disk. Glass-to-metal seals are created by cooling the glass and the metal from a high temperature, during which the metal, with a larger coefficient of thermal expansion (CTE), shrinks more than the glass. When the metal shrinks more than the glass, the glass is put in state of compression which can protect the glass from mechanical loads and guarantees a robust, mechanically insensitive seal. Understanding the glass stress state is critical to designing a robust hermetic connector.

Glass-to-metal seal designers have relied on finite-element analysis (FEA) for many years [1, 2]. Years of analysis have shown that reliable product designs require models that can accurately predict the response of the sealing glass to mechanical and temperature loadings over prolonged periods. Finite-element analysis has been used to optimize the stress state in the glass during the design process and understand the stress state when glass cracking has been observed. To date, finite-element analysis of a GTMS has not been validated. This paper will summarize an effort to perform validation of a GTMS seal finite-element model.

A common material pair used in glass-to-metal seals is Schott 8061 alkali-silicate glass and 304L VAR stainless steel. This material combination has been shown to provide effective hermeticity for long-term applications. Recently, both of these materials have been extensively characterized in the strain and temperature regime associated with glass-to-metal sealing, i.e. small plastic strains and across a large temperature range. A nonlinear viscoelastic material model has been calibrated for Schott 8061 [3] and material data has been taken for 304L VAR stainless steel over small strains and temperature regime of interest [4]. The newly calibrated material models have been applied to a GTMS finite-element model. The evolution of material models and model predictions will be shown.

To validate the finite-element model, the residual stress in a simple, concentric GTMS was measured using the indentation fracture method [5-7]. The stress on the surface of a GTMS seal was mapped using the indentation fracture method. Model predictions were compared to measured data. Analysis of the comparison is provided to evaluate the validity of the finite-element model.

2. EXPERIMENTAL RESULTS

An assortment of data has been measured as part of the effort to validate the GTMS finite-element model. In an effort to observe creep below the glass transition temperature, bars of glass were subject to 3-point bend at room temperature over a long period of time. A simple, concentric GTMS was designed and fabricated to be used for modeling and experimental purposes. The indentation fracture method was used to infer the residual stress on the surface of the glass in the simple concentric seal.

2.1. Room Temperature Creep

After the development of the thermo-viscoelastic Schott 8061 material model [3], low temperature creep experiments were performed to provide additional data for model evaluation. It was found that subjecting glass bars to high loads over a long period of time will cause permanent deformation due to structural relaxation in the glass. A series of low temperature creep tests were performed to observe structural relaxation in the glass.

A photo a glass bar subject to 3-point bend loading is shown in Figure 1. A load was applied to the specimen by placing weights on the rounded cylinder. The glass bar was annealed and then its shape was measured using a profilometer prior to loading. A load was applied such that the maximum bending stress in the glass was nominally 27 MPa. The load was held constant for approximately six months. After the specimen was removed from the test fixture, the shape of the bar was again measured using a profilometer. The difference between the pre-test and post-test measurements provide the permanent deflection in the glass.

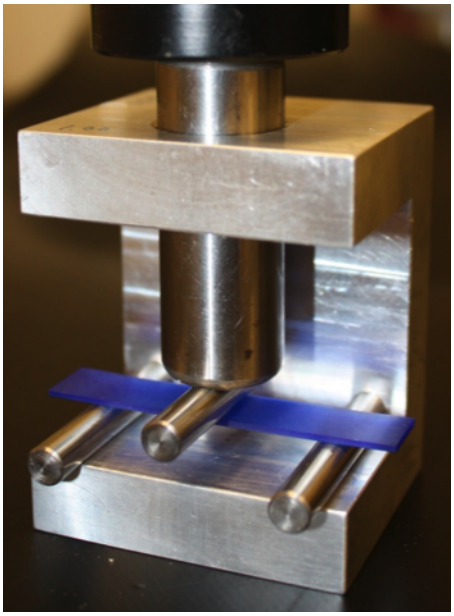

Figure 1. Photo of Schott 8061 Bend Bar Subject to 3-Point Bend Dead Load at Room Temperature.

In the first iteration of these tests, two samples were loaded for six months and the permanent deformation measured. In a second iteration of these tests one additional solid glass bar was loaded at a nominal stress of 24 MPa for approximately 3 months. The measured permanent vertical displacement in the glass bars subjected to room temperature dead loads are shown in Figure 2.

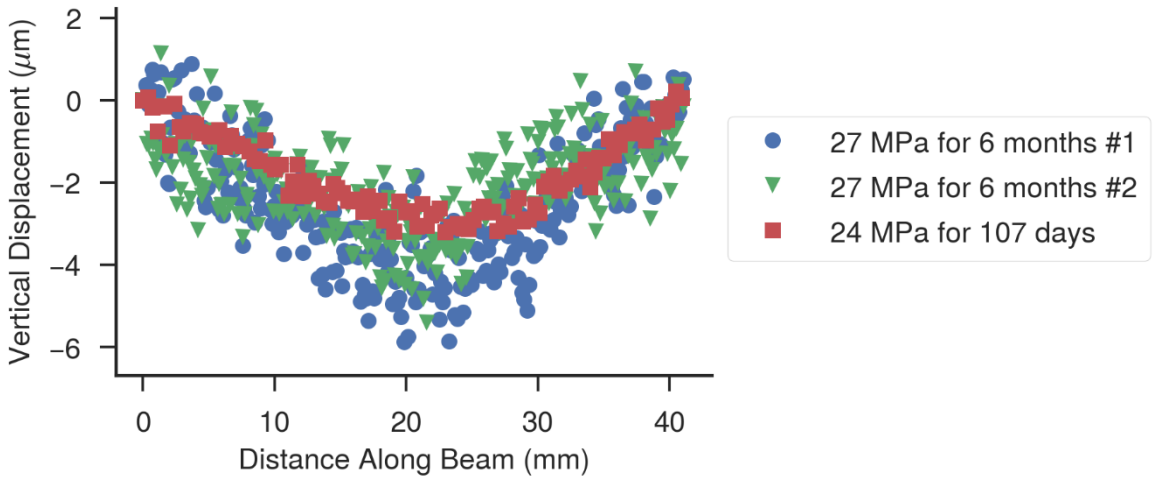

Figure 2. Measured Permanent Vertical Displacement in Solid Schott 8061 Glass.

As seen in Figure 2, there was measurable creep in the solid glass bars at 440 °C below the glass transition temperature. There is obvious uncertainty in the measurements. At any given location along the length of a single specimen, the measured displacement can vary up to 4 μm or nearly 70% of the peak displacement. Though uncertainty exists, these data show that structural relaxation does indeed occur at temperatures far below the glass-transition temperature. Further investigation and refinement of the experimental technique could potentially provide higher-fidelity data.

2.2. Measuring Residual Stress

Measuring the residual stress in the glass is critical to validating the GTMS finite-element model. Various experiments such as material removal, indentation fracture, and digital image correlation methods were evaluated to determine which could most effectively and accurately measure the residual stress in a GTMS [8, 9]. Stress mapping using the indentation fracture method was proven to be a reliable technique to measure the residual stress in a GTMS.

2.2.1. Simple Concentric Seal

A simple, concentric GTMS was created to use for model validation purposes. This geometry is much simpler than most GTMS geometries. The shell, or the metal ring surrounding the glass, is 304L VAR stainless steel. The glass is a solid preform of Schott 8061. The seal is created using a typical glass sealing cycle. The shell's outer diameter is nominally 16 mm and the inner diameter is nominally 10.8 mm. The

thickness of the concentric seal is nominally 3 mm. A photo of the concentric seal is shown in Figure 3. Further information regarding fabrication of this concentric seal is provided in [10].

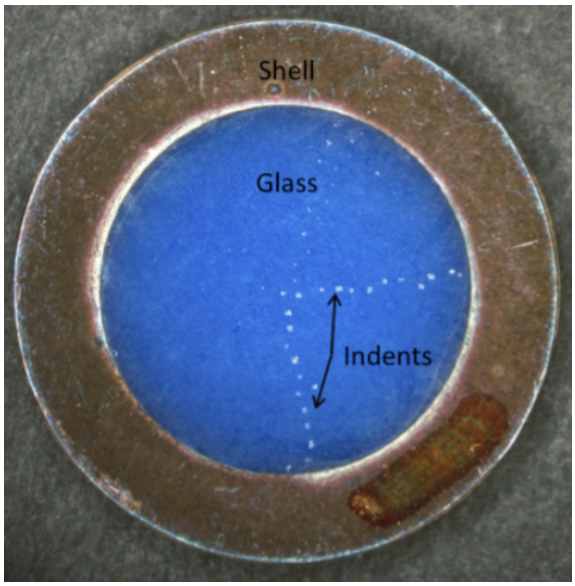

Figure 3. Photo of the Concentric Glass-to-Metal Seal Used for Validation Purposes.

2.2.2. Indentation Fracture Method Results

The indentation fracture method uses a Vickers indenter to induce cracks in the glass. The Vickers indenter is aligned such that the cracks propagate in the radial and hoop directions in the concentric seal. Comparing crack lengths in unstressed and stressed glass enables inference, i.e. derived "measurements", of the radial and hoop stresses on the surface of the glass. A thorough discussion of the method and results are available in [10].

Residual stress in the glass were measured on four samples of the concentric seal geometry. A summary of the samples is shown in Table 1. The four samples were made between January and May 2015 and tested in April or December 2015. The effects of oxidizing the metal prior to sealing the GTMS were investigated in samples #1 and #2. It was found that oxidizing the metal had little effect on the residual stress measurements. The effects of polishing the surface of the GTMS prior to indentation was investigated in samples #3 and #4. The shells in both of these samples were oxidized. It was discovered that polishing the GTMS prior to testing resulted in a more consistent stress measurement.

As outlined in [10], the residual stress can be inferred from the length of the cracks emanating from the Vickers indentation. The measured radial and hoop stresses on the surface of the glass in the concentric seal geometry are shown in Figure 4 and Figure 5.

Table 1. Disposition of the Concentric Seal Samples Tested Using Indentation Fracture Method.

Sample	Sealing Date	Testing Date	Polished?	Oxidized?
1	January 2015	April 2015	Yes	Yes
2	January 2015	April 2015	Yes	No
3	March 2015	December 2015	Yes	Yes
4	May 2015	December 2015	No	Yes

The radial and hoop stress measurements follow the same trends sample-to-sample. For the radial stress, sample #4 shows the most variation as compared to samples #1 through #3. Though sample #2 shows large apparent variation in radial stress at $r > 5$ mm, this sharp decrease in stress is due to compression immediately at the interface and is consistent with predictions shown later (Figure 10). The variation in sample #4 is believed to be due to the surface of the glass not being polished. The hoop stress measurements of sample #4 across the entire seal and sample #2 near the glass-to-metal interface appear to vary widely from measurement to measurement.

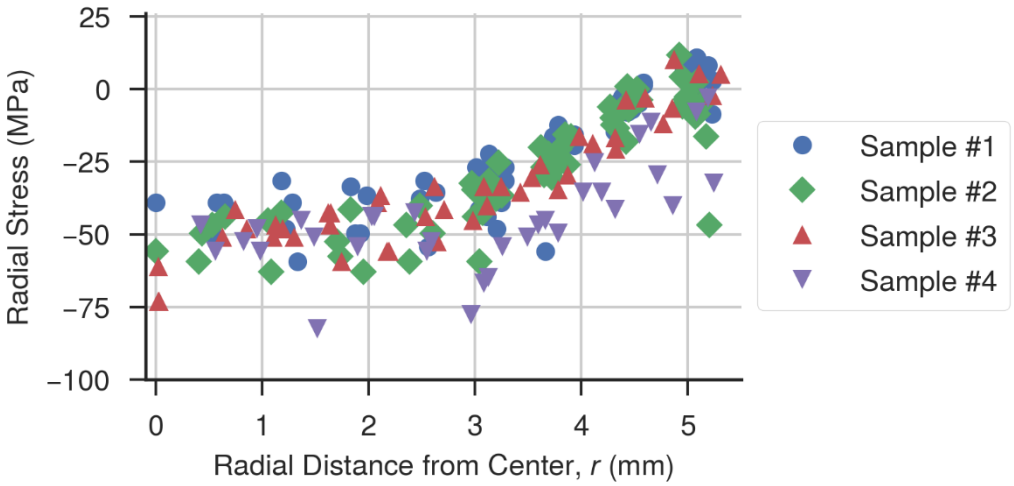

Figure 4. Measured Radial Stress in the Glass for Four Samples of the Concentric Seal Geometry.

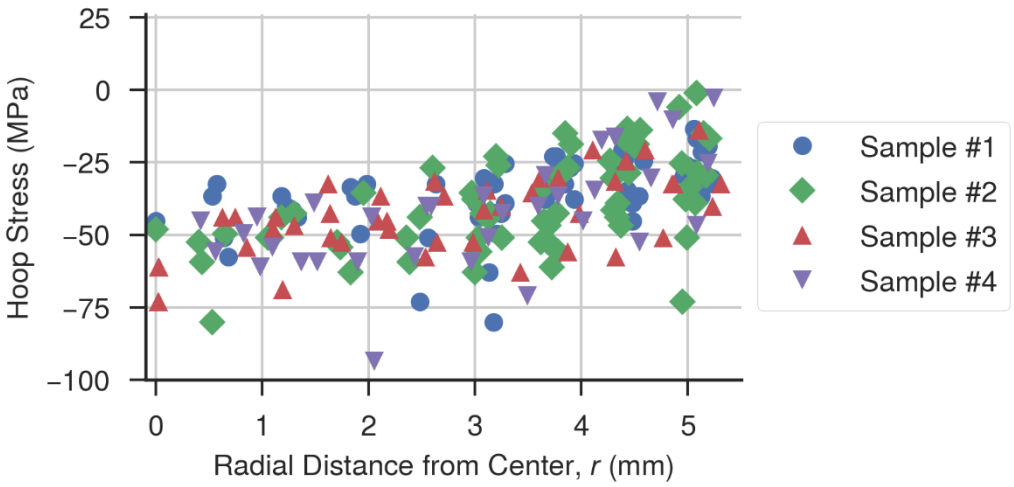

Figure 5. Measured Hoop Stress in the Glass for Four Samples of the Concentric Seal Geometry.

2.2.3. Analysis of Residual Stress Results

A statistical analysis was performed on the residual radial and hoop stress measurements. In this analysis, a mean response as well as tolerance intervals were calculated. Due to the observed variation in measured residual stress in the unpolished sample, only samples that were polished prior to indentation were included in this analysis. Furthermore, only data away from the center and the material interface were included. Specifically, measurements with $r < 0.25$ mm and $r > 5.0$ mm were excluded from the data set. This data was excluded to avoid any edge effects and inconsistencies observed near the center of the glass ($r = 0$).

The data set was further reduced into two subsets, split at $r \approx 2.5$ mm. For the measured radial stress, at approximately $r \approx 2.5$ mm, there is a distinct change in the shape of the overall response. The hoop stress exhibits similar behavior though not as strongly. The hoop stress data was split at approximately $r \approx 2.75$ mm.

A linear regression was performed on each subset to determine the mean response as well as 95/90 tolerance bounds. The bounds were calculated such that there is 90% confidence that 95% of an infinite amount of further data sampled would be captured within the dashed lines (tolerance bounds). For both the radial and hoop stress, the mean and tolerance intervals bound the data well. The reduced radial and hoop data are shown in Figure 6 and Figure 7. These reduced data sets will be used when making comparisons to model predictions in Section 4.

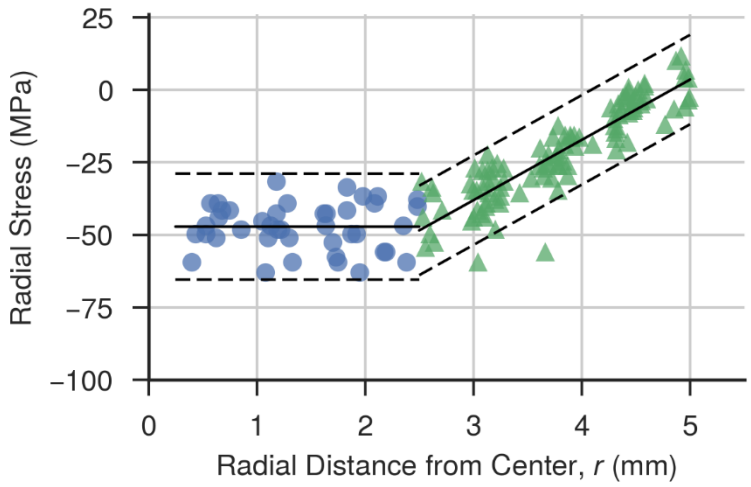

Figure 6. Reduced Data Set of the Measured Radial Residual Stress. Solid Lines are the Mean and Dashed Lines are the 95/90 Tolerance Bounds.

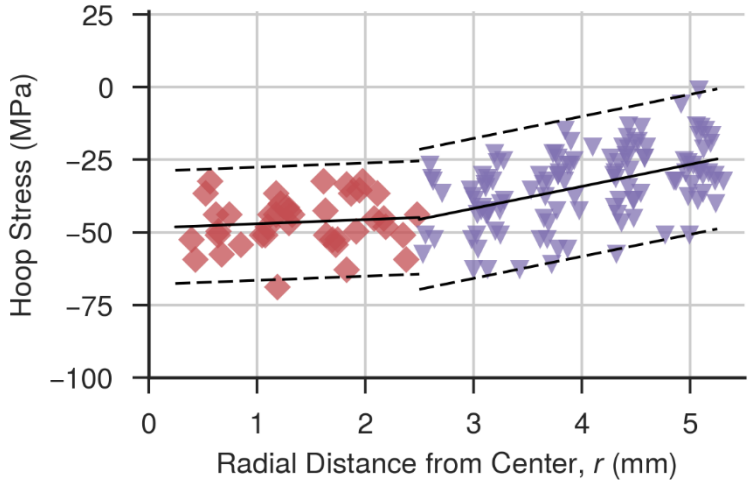

Figure 7. Reduced Data Set of the Measured Hoop Residual Stress. Solid Lines are the Mean and Dashed Lines are the 95/90 Tolerance Bounds.

3. FINITE-ELEMENT MODEL

There has been an evolution of GTMS models used at Sandia over the last couple of decades [11, 12]. Material models and modeling assumptions have improved. A finite-element model of the concentric GTMS shown in Figure 4 was created in order to perform GTMS model validation. The model boundary conditions and mesh are described. The glass material models have evolved from simply elastic to thermoelastic to thermo-viscoelastic. The material models for the stainless steel have evolved from multi-linear thermoelastic-plastic to elasto-viscoplastic. An overview of the material models for the glass and stainless steel is provided, including material model calibrations. Finite-element model results will be shown in the following section.

3.1. Model Description

The concentric seal was designed such that the geometry was simple and easy to model. Since the geometry of the concentric seal is symmetric, an axisymmetric finite-element model was used. Furthermore, through thickness symmetry was also used in the model. A schematic of the finite-element model used is shown in Figure 8. Only the upper-right portion of the geometry is actually modeled.

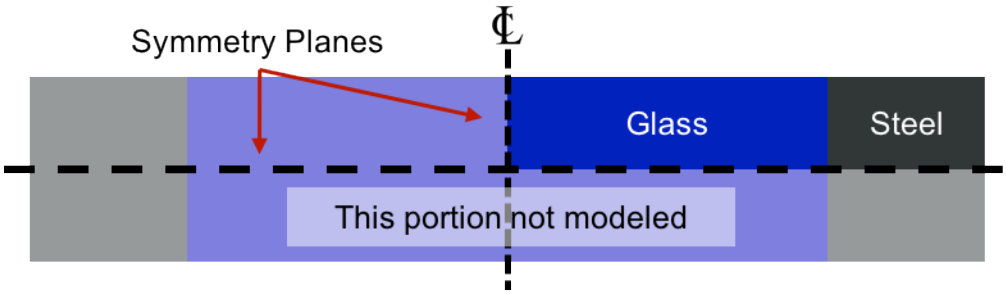

Figure 8. Cross-Section of the Concentric Seal Model Showing the Symmetry Planes.

A uniform temperature boundary condition was applied to the entire model. The model was cooled at 2 °C/min from 600 °C to room temperature. Fixed boundary conditions were applied to all symmetry planes as well as along the center axis. The interface between the glass and steel is assumed to be perfectly bonded. The model has 30,298 uniform-gradient hexahedral elements and 36,620 nodes. Mesh sensitivity has been investigated previously [13] and showed that the mesh density used in this report is converged.

3.2. Schott 8061 Glass

Schott 8061 is an alkali-silicate glass that contains barium produced by Schott and used by the hermetic connector industry in glass-to-metal seals. Schott 8061 can be produced as a solid preform and or press-powdered preform. In this study, only the solid Schott 8061 was considered.

For many years, the glass was modeled using a thermoelastic (TE) material model which is described in detail in [12, 14]. This model assumes a constant CTE from 460

°C to room temperature. Temperature dependent Young's modulus was included over the same temperature range.

Viscoelastic material data were obtained for Schott 8061 circa 2014. The data were used to calibrate the Simplified Potential Energy Clock (SPEC) model that is described in [15]. The SPEC material model is based on the Potential Energy Clock (PEC) which is described in [16, 17]. The calibration and validation of the SPEC model applied to Schott 8061 is outlined in [3]. Chambers et al. showed that the SPEC material model can accurately represent the behavior of Schott 8061 across multiple temperatures and rates.

3.3. 304L VAR Stainless Steel

304L stainless steel is an alloy commonly used by the hermetic connector industry that pairs well with Schott 8061 glass. The combination of these materials results in a compression-based GTMS. 304L stainless steel is a low carbon version of 304 that has favorable weld properties. 304L VAR is used in high consequence systems due to the increased quality of the alloy.

Similar to the glass models, 304L material models for GTMS have evolved over the years. The most common material model used for 304L has been a multi-linear thermoelastic-plastic model (MLTEP) which was calibrated to large plastic strain data. The 304L stainless steel multi-linear thermoelastic-plastic material model used for GTMS simulation is described in [8, 12, 14]. The combination of thermoelastic glass and multi-linear thermoelastic-plastic material models make up what is referred to as "legacy" material models.

For the present discussion, we employ a rate- and temperature-dependent elasto-viscoplastic model described in [18, 19]. The model was calibrated to tensile and stress relaxation data at various controlled temperatures ranging from -55 °C to 500 °C and available at two nominally quasi-static straining rates, 3.1e-05 and 3.1e-06. The characterization tests loaded the specimens quasi-statically, then held the applied displacement while measuring the load drop-off. The available characterization data was collected by Bonnie Antoun and is described in [4, 8]. The model was originally calibrated by a subject matter expert to the room temperature, 300 °C, and 500 °C data taken at the lower strain rate, with strain-rate dependence according to the observed relaxation [20]. Subsequently, the model was shown to predict the response of the faster strain-rate data. Figure 9 plots the characterization data used as well as the model calibration. At a later date, the temperature-dependent yield function was re-calibrated to the -55 °C data when it became available. The model is currently stored in a Git repository for version control accessible at: https://code-source.sandia.gov/git/sierraMaterialModels/.

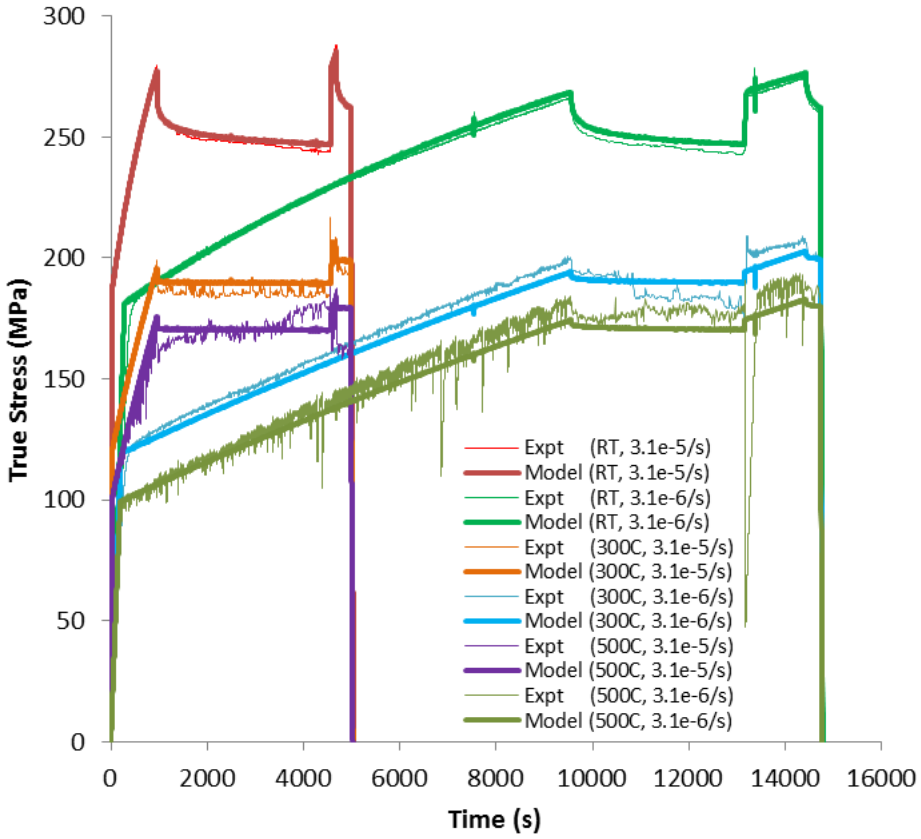

Figure 9. Rate and Temperature Characterization Data and The Output from Model Calibration for 304L VAR Stainless Steel.

4. MODEL COMPARISON

Validation of the GTMS finite-element model is based on a comparison of the residual stress measurements and deterministic model predictions from calibration to one material data set. Therefore the model does not predict the effects of any stochastic material variability that exists in the data sets (but comingled with random noise in the inferred/derived stress measurements). For expediency here, preliminary validation comparisons are made between deterministic model predictions and the populations of inferred data measurements. More formal validation of the model would involve accounting for material variability in the model calibration and predictions and then validating against the data population tolerance bounds as demonstrated in [20, 21].

A series of predictions were made with the GTMS finite-element model. These predictions included different material models, boundary conditions, and aging of the glass-to-metal seal. It will be shown that the evolution of material models and modeling strategies improve the residual stress predictions.

Model predictions of the residual stress along the surface of the glass will be compared to residual stress measurements. Figure 10 provides a depiction of the residual stress in the axisymmetric GTMS model. As can been seen in the image, residual stress is extracted from the row of elements on the symmetry plane (the plane of the page) on the free surface of the glass. Recall, the bottom of each contour image is a symmetry plane in the thickness direction and the symbol ℄ represents the center axis of the GTMS. Comparisons are not made for the steel as residual stress data is not currently available.

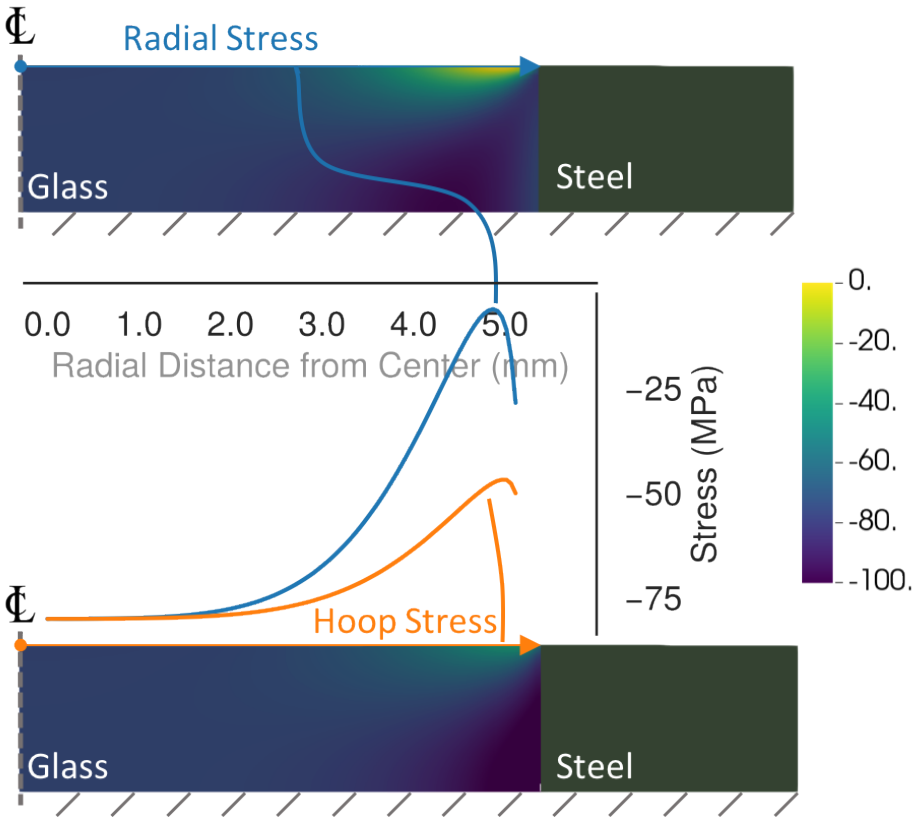

Figure 10. Residual Radial and Hoop Stress in the Glass of the GTMS at Room Temperature.

4.1. "Legacy" Material Models

The GTMS finite-element model is first evaluated using the thermoelastic glass and multi-linear thermoelastic-plastic steel material models. Comparisons of the radial and hoop residual stress data and model predictions are shown in Figure 11 and Figure 12. In these figures, data are symbols and the solid-colored lines are model predictions. Solid and dashed black lines represent the mean and 95/90 tolerance intervals of the measured data.

In both cases, the model over predicts the compression along most of the surface of the GTMS. Near the glass-to-metal interface, the radial stress prediction lies in the center of the measured data. At the same location, the hoop stress prediction is within the tolerance intervals of the data, but far from the mean of the data (as the most consistent quantity hear to compare the deterministic results to). With these material models, the model only appears to be valid (as a mean predictor) for the radial stress near the glass-to-metal interface. For the simple geometry, this difference between model and predictions may have little consequence. If electrical contacts were included, the compression on the electrical contacts would be too large, leading to increased stress in the contact.

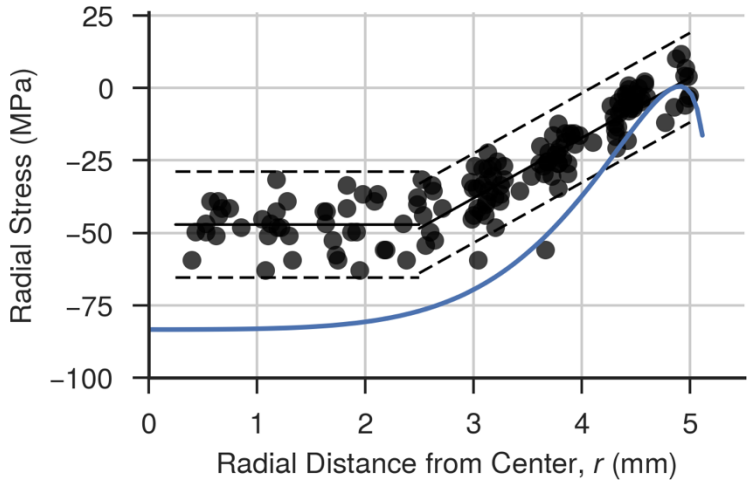

Figure 11. Comparison Between Measured Radial Stress and Model Predictions with Thermoelastic Glass (TE) and Thermoelastic-Plastic Steel (MLTEP).

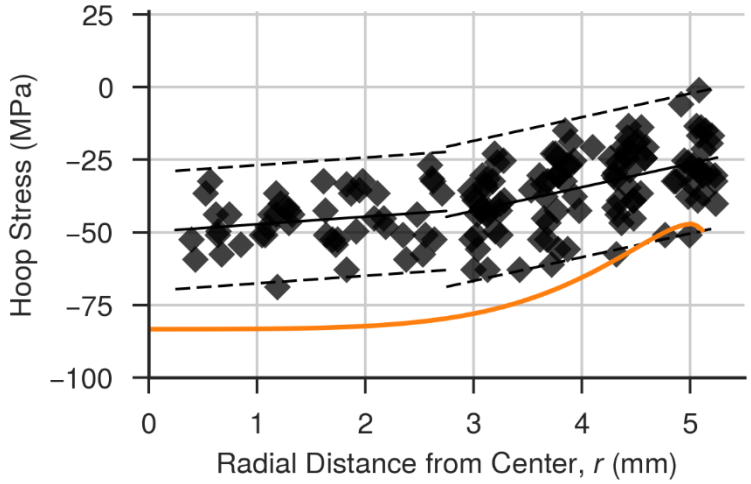

Figure 12. Comparison Between Measured Hoop Stress and Model Predictions with Thermoelastic Glass (TE) and Thermoelastic-Plastic Steel (MLTEP).

4.2. Rate-Dependent Material Models

The material models used previously do not include the rate/material effects of the glass (viscoelastic effects) or the steel (strain-rate dependence). The thermo-viscoelastic glass (SPEC) and viscoplastic steel (BCJ) material models include the rate effects of both materials. A comparison of the measured residual stress and the model predictions for the radial and hoop stress are shown in Figure 13 and Figure 14. In these figures, data are symbols and the colored lines are model predictions. Solid and dashed black lines represent the mean and 95/90 tolerance intervals of the measured data.

The trends observed in the comparison between model predictions and measured data do not change significantly with the addition of rate/material effects. The model predicts less compression in both the radial and hoop directions. In both the radial and hoop directions, the predicted stress at the center of the GTMS decreased by 9%. Though the predicted compression decreased, the model still overpredicts the compression at the center of the seal. At the glass-to-metal interface, the radial stress prediction is within 2 MPa of the thermoelastic predictions and near the mean of the data. The predicted hoop stress at the glass-to-metal interface is now within the tolerance bands of the measured data but still far from the mean of the data.

The change in model predictions are due to a combination of effects. The data used to populate both of the rate-dependent models have been meticulously collected such that they are more representative of temperatures the material will experience (annealed vs non-annealed, etc.). The viscoelastic glass model has higher fidelity across the temperature range of interest. Also, both material models allow for structural relaxation (glass) and creep (steel) to occur. The combination of these effects result in lower compression at the center of the GTMS.

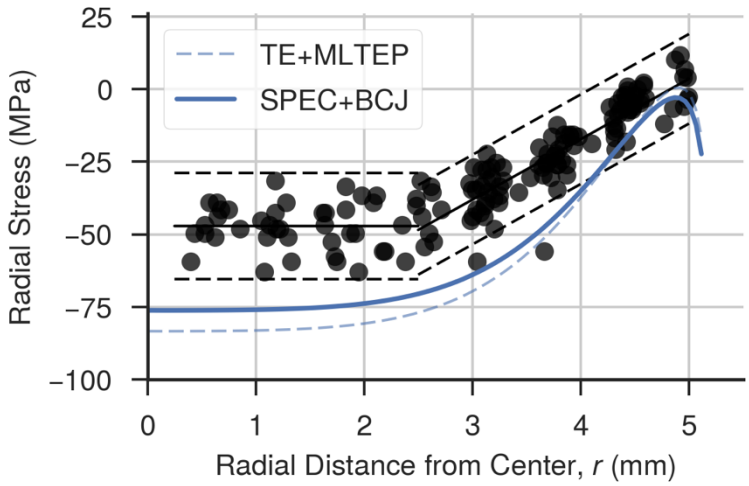

Figure 13. Comparison Between Measured Radial Stress and Model Predictions with Thermo-Viscoelastic Glass (SPEC) and Viscoplastic Steel (BCJ).

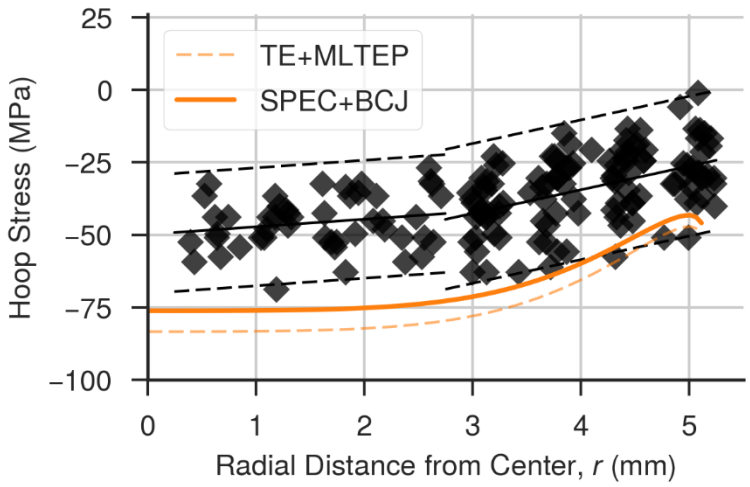

Figure 14. Comparison Between Measured Hoop Stress and Model Predictions with Thermo-Viscoelastic Glass (SPEC) and Viscoplastic Steel (BCJ).

4.3. Modeling Assumption Uncertainty

Though the rate-dependent material models offer advanced capabilities over the "legacy" material models, the model predictions with rate-dependent models are not a substantial improvement when compared to measured data. As both the SPEC glass model and the BCJ steel models have been validated under representatively similar conditions (Section 3.2 and Section 3.3), it was theorized that perhaps the GTMS model was not accurately representing the physical GTMS. Possible sources of model error include model cooling rate, the glass-to-metal interface, polishing of the GTMS during indentation testing, and accounting for the time between GTMS sealing and testing. These varying conditions were analyzed to investigate the effect on predicted residual stress.

First, the effect of cooling rate on model predictions was investigated. Figure 15 shows the predicted residual radial and hoop stress for cooling rates of 2 °C/min, 3 °C/min, and 10 °C/min. As can be seen in the image, there is little difference between the residual stress for different cooling rates. The maximum difference between cooling rates is less than 2% for both the radial and hoop stress predictions. Based on these results, the model prediction is insensitive to the cooling rate.

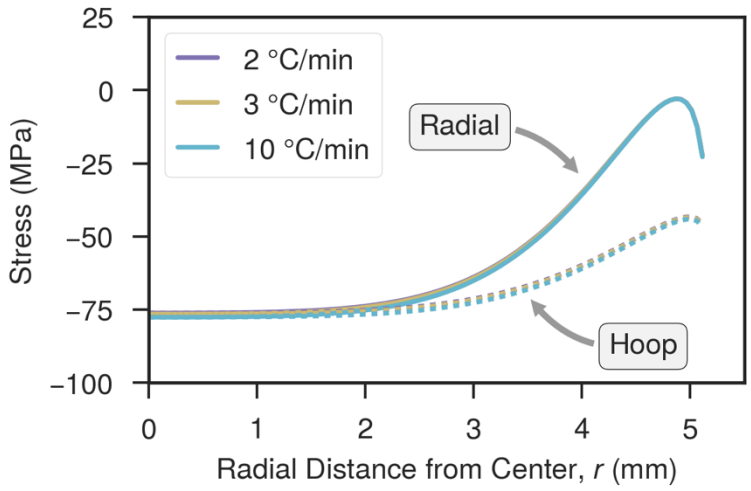

Figure 15. Model Predictions of Residual Radial and Hoop Stress for Different Cooling Rates.

The effect of the glass-to-metal interface model assumption was investigated next. The baseline model assumes the interface is perfectly bonded, i.e. at the interface the two materials share nodes. The model was modified to allow contact at the glass-to-metal interface with a constant coefficient of friction of 0.3. The predicted residual radial and hoop stress on the surface of the glass for a perfectly bonded and constant friction interface are shown in Figure 16. In this image, the solid lines are the radial stress and the dashed lines the hoop stress. At the center of the GTMS, the model prediction is insensitive to the interface condition. At the glass-to-metal interface, both the radial and hoop stress predictions are significantly different. The radial stress decreases by approximately 60 MPa and the hoop stress decreases by approximately 30 MPa.

When compared to measured data, the perfectly bonded interface assumption is a better representation of reality. When the GTMS is produced, the Schott 8061 glass does not chemically bond to the 304L stainless steel. Though glass does not bond to the shell, while the glass is above the glass transition temperature the viscosity is low enough that it can flow to conform to the shape of the metal shell. The current model does not capture that physical behavior. Because of this, and the large amounts of compression that exists in the compression seal, the perfectly bonded interface is a better modeling approach.

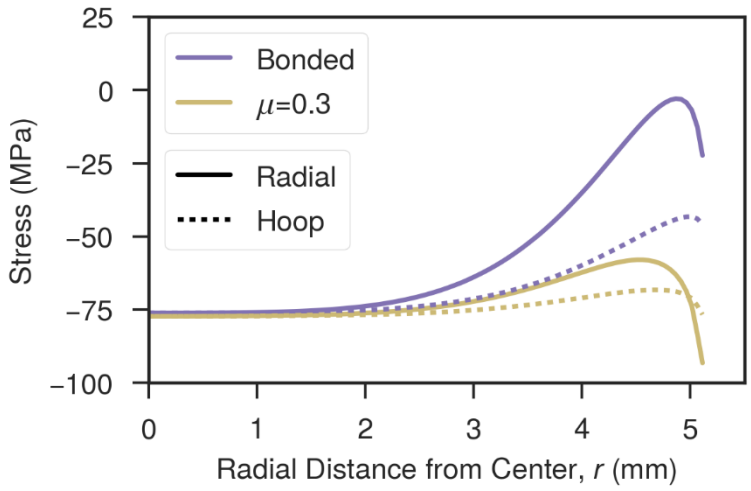

Figure 16. Model Predictions of Residual Radial and Hoop Stress for Perfectly Bonded and Constant Friction Material Interface.

Neither the model cooling rate or glass-to-metal interface assumption led to an improvement in the predicted residual stress. The effects of polishing and aging the GTMS were investigated next. As shown in Section 2.1, structural relaxation was observed in Schott 8061 at room temperature over a period of approximately six months. If structural relaxation occurred in a stressed bar over that time frame, it was theorized that structural relaxation could occur in a GTMS over the same period. A series of models were created to investigate the effects of polishing and aging.

In this series of models, the cooling rate is 2 °C/min and the interface is assumed to be perfectly bonded. After the model reaches room temperature, the temperature is held constant for six months (the average wait between seal manufacturing and testing). After the six months hold time, the top layer of elements was removed via element death. This last step simulates the polishing process that was carried out prior to indentation fracture testing.

Figure 17 and Figure 18 show the radial and hoop stress predictions compared to the measured data. The figure shows the evolution of the material and modeling assumptions. The thick-solid lines show the combination of rate-dependent material models, aging the GTMS for six months, and polishing the top surface. In both the radial and hoop directions, the model predictions now lie within the tolerance intervals of the data across the entire surface of the glass, but are biased low relative to the experimental mean curves as the most relevant comparison quantity. The predicted radial stress follows the bottom tolerance interval until approximately $r = 4.5$ mm. The predicted hoop stress behaves similarly, following the bottom tolerance interval until approximately $r = 3.0$ mm.

During the analysis, it was discovered that the combination of both aging and polishing were required to make the predicted residual stress fall within the measured data. Including the aging effects had the largest impact on the predicted residual stress, decreasing the predicted compression by 20%.

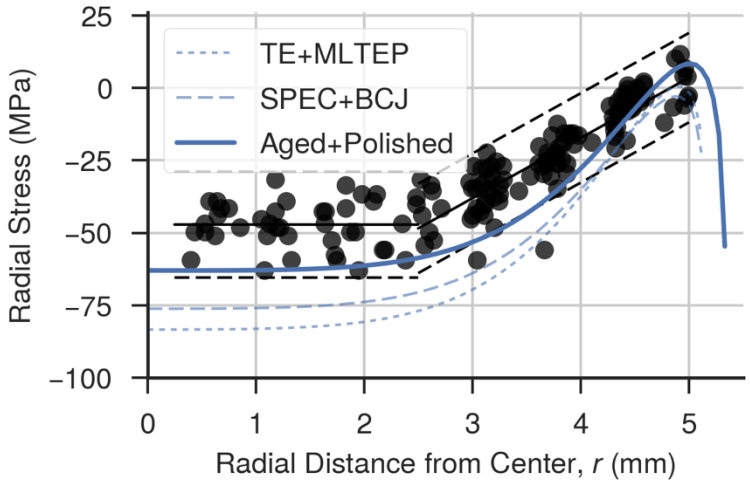

Figure 17. Comparison Between Measured Radial Stress and Model Predictions After Aging and Polishing the GTMS.

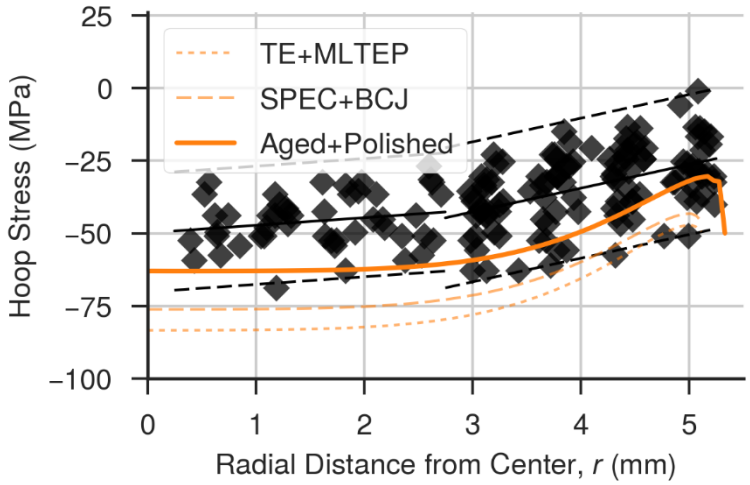

Figure 18. Comparison Between Measured Hoop Stress and Model Predictions After Aging and Polishing the GTMS.

4.4. Model Validation Overview

The progression of the GTMS model described above show that the model has evolved to be able to predict residual stress that lies within measured data, but is biased low relative to the mean experimental results as the most relevant comparison quantity. A few key findings were found through the model evolution. First, the model predicts higher compression at the center of the GTMS as compared to the measured data. As discussed in [10], the indentation fracture method of inferring residual stress is more sensitive to the accuracy of the crack length measurement in compression than in tension. This means that a small error in measuring the crack length near the center of the glass could cause a larger error in the calculated stress. This sensitivity to

measured crack length is likely a contributing factor to the large distribution in the derived measurements of residual stresses, particularly compressive stresses.

Second, as shown in Figure 19 model predictions are most sensitive to the aging of the GTMS. If the GTMS model is not aged, the predicted residual stress values more substantially overpredict the data except at the glass-to-metal interface. Based on these results, it is recommended to include aging of a hermetic connector in an analysis. In a hermetic seal with an electrical contact, the increased compression would lead to added stress applied to the contact. Overpredicting the compression near an electrical contact could lead to overpredicting the plastic strain that could occur in a softer alloy, such as Alloy 52.

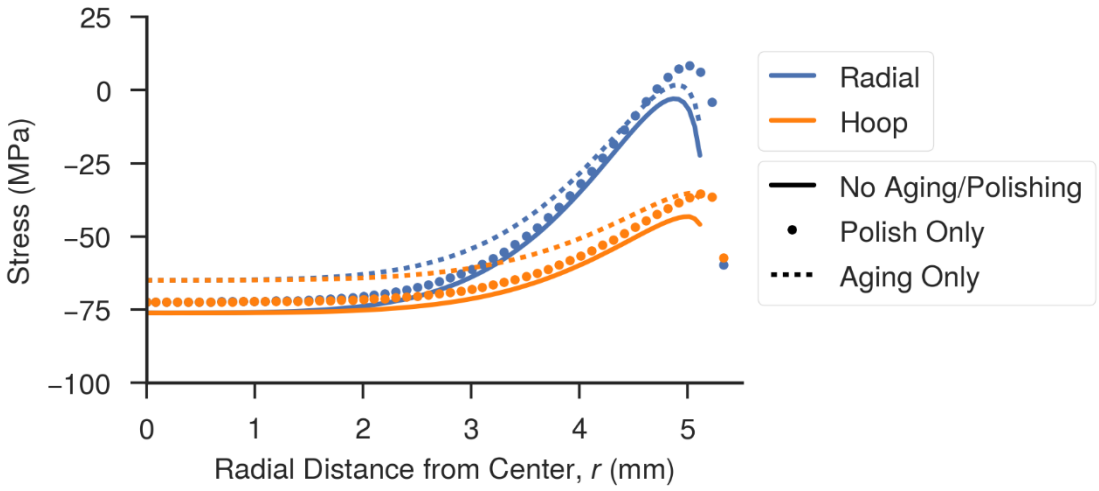

Figure 19. Model Predictions of Residual Radial and Hoop Stress Showing the Effect of Aging and Polishing.

Last, the model predictions best match the measured data near the glass-to-metal interface. The predicted residual radial stress at the glass-to-metal interface ($r \approx 5$ mm) shows less sensitivity to material model and boundary condition assumptions than the center of the GTMS. When including aging and polishing, the model predicts the mean of the measured data near the material interface. The analysis also showed that a perfectly bonded interface provides a more accurate prediction of the stress at the interface.

In summary, the GTMS finite-element model that includes rate-dependent material models and aging effects is valid within the variation of the measured data. Though the indentation fracture method residual stress results are not exact, the model predictions fall within the calculated 95/90 tolerance bounds at the center of the seal and matches the mean measurement near the glass-to-metal interface. Based on these results, the model is assessed to be valid for predicting mean behavior near the glass-to-metal interface for this use case.

5. CONCLUSIONS

Finite-element modeling is a critical tool when designing glass-to-metal hermetic connectors. A simple GTMS was made for the purpose of measuring the residual stress on the surface of the glass. The indentation fracture method was used to infer the stress on the surface of the glass in the GTMS. Such derived measurements were made at various locations, providing a stress map of the surface. A finite-element model of the concentric seal was analyzed. It was shown that including rate-dependent material models, accounting for the age of the seal, and accurately representing the testing process resulted in deterministic model predictions that fall within 95/90 tolerance bounds of the data, but expect near the regions of tension in the glass are biased low relative to the mean experimental results as the most relevant comparison quantity. Based on the results shown in this paper, the finite-element model is shown to be most valid for predicting the glass mean residual stress state in regions of tension on the surface of the glass.

REFERENCES

1. A. K. Varshneya, R. J. Petti, Finite element analysis of stresses in glass-to-metal foil seals. *J. Am. Ceram. Soc.*, Volume 61, 1978, Pages 498–503.
2. D. Lei, Z. Wang, J. Li. The analysis of residual stress in glass-to-metal seals for solar receiver tube. *Mater. Des.*, Volume 31, 2010, Pages 1813–1820.
3. R. S. Chambers, R. Tandon, M. E. Stavig. Characterization and calibration of a viscoelastic simplified potential energy clock model for inorganic glasses. *J. Non-Cryst Solids*, Volume 432, 2016, Pages 545-555.
4. B. R. Antoun, R. S. Chambers, J. M. Emery, R. Tandon. Small strain plasticity behavior of 304L stainless steel in glass-to-metal seal applications. Challenges in Mechanics of Time-Dependent Materials, Volume 2: Proceedings of the 2014 Annual Conference 49 on Experimental and Applied Mechanics, Conference Proceedings of the Society for Experimental Mechanics Series. The Society for Experimental Mechanics, Inc., 2015.
5. D. B. Marshall, B. R. Lawn. An indentation technique for measuring stresses in tempered glass surfaces. *J. Am. Ceram. Soc.*, Volume 60, 1977, Pages 86–87.
6. D. B. Marshall, B. R. Lawn. Residual stress effects in sharp contact cracking Part 1 Indentation fracture mechanics. *J. Mater. Sci.*, Volume 14, 1979, Pages 2001–2012.
7. D. B. Marshall, B. R. Lawn, P. Chantikul. Residual stress effects in sharp contact cracking Part 2 Strength degradation. *J. Mater. Sci.*, Volume 14, 1979, Pages 2225–2235.
8. R.S. Chambers, J.M. Emery, R. Tandon, B.R. Antoun, M.E. Stavig, C. Newton. Characterization & modeling of materials in glass-to-metal seals: Part I. SAND2014-0192, Sandia National Laboratories, Albuquerque, NM, January 2014.
9. R.S. Chambers, J.M. Emery, R. Tandon, B.R. Antoun, M.E. Stavig, C. Newton, C. Gibson, D. Bencoe. Proposed testing to assess the accuracy of glass-to-metal seal stress analyses. SAND2014-17881, Sandia National Laboratories, Albuquerque, NM, September 2014.
10. T. Buchheit, K. Strong, C. Newton, T. Diebold, D. Bencoe, M. Stavig, R. Jamison. Stress mapping in glass-to-metal seals using indentation crack lengths. SAND2017-9013, Sandia National Laboratories, Albuquerque, NM, August 2017.
11. E. Beauchamp, S. Burchett. Techniques of seal design. Ceramics and Glasses, S. J. Schnider, Vol. 4 of Engineered Materials Handbook, ASM International, 1991.
12. R. Jamison, B. Elisberg, J. Christensen. Finite element analysis of Glenair hermetic LJT connector designs. SAND2015-4457, Sandia National Laboratories, Albuquerque, NM, June 2015.
13. A. Gullerud, J. Emery, R. Jamison. Computational assessment of brittle fracture in glass-to-metal seals. ASME International Mechanical Engineering Congress and Exposition, Volume 9: Mechanics of Solids, Structures and Fluids:161-169, 2010.

14. B. Elisberg, R. Jamison, J. Christensen. Finite element analysis of SA4073 hermetic LJT connector designs. SAND2016-10417, Sandia National Laboratories, Albuquerque, NM, October 2016.

15. D. B. Adolf, R. S. Chambers, M. A. Neidigk. A simplified potential energy clock model for glassy polymers. *Polymer*, Volume 50, Issue 17, 2009, Pages 4257-4269.

16. J. M. Caruthers, D. B. Adolf, R. S. Chambers, P. Shrikhande. A thermodynamically consistent, nonlinear viscoelastic approach for modeling glassy polymers. Polymer, Volume 45, 2004, Pages 4577-4597.

17. D. B. Adolf, R. S. Chambers, J.M. Caruthers. Extensive validation of a thermodynamically consistent, nonlinear viscoelastic model for glassy polymers. *Polymer*, Volume 45, 2004, Pages 4599-4621.

18. D. J. Bamman, M. L. Chiesa, G. C. Johnson. Modeling large deformation and failure in manufacturing process. In T. Tatsumi, E. Watanabe, and T. Kambe, editors, Theoretical and Applied Mechanics. Elsevier Science, 1996.

19. A. A. Brown and D. J. Bammann. Validation of a model for static and dynamic recrystallization in metals. *Int. J. Plasticity*, 32–33, 2012, Pages 17 – 35.

20. R. Jamison, V. Romero, M. Stavig, T. Buchheit, C. Newton. Experimental data uncertainty, calibration and validation of a viscoelastic potential energy clock model for inorganic seal glasses, ASME Verification & Validation Symposium, Las Vegas, NV, 2016.

21. R. Jamison, B. Elisberg, K. Troyer, M. Stavig, K. Ewsuk. Assessing sealing glass equivalency based on viscoelastic behavior. The 12th Pacific Rim Conference on Ceramic and Glass Technology, Waikoloa, HI, 2017.

DISTRIBUTION

1	MS0346	Kurtis Ford	Org. 01556
1	MS0346	Diane Peebles	Org. 01556
1	MS0346	Brenton Elisberg	Org. 01556
1	MS0346	Scott Grutzik	Org. 01556
1	MS0523	Kevin Ewsuk	Org. 02631
1	MS0781	Mark Retter	Org. 06621
1	MS0825	Jeff Payne	Org. 01513
1	MS0828	Walter Witkowski	Org. 01544
1	MS0840	Kevin Long	Org. 01554
1	MS0840	Eliot Fang	Org. 01554
1	MS0889	Antoun Sumali	Org. 01851
1	MS0889	Dave Reedy	Org. 01556
1	MS0889	Kevin Strong	Org. 01851
1	MS1168	Steven Wix	Org. 01356
1	MS1411	Mathias Celina	Org. 01853
1	MS0899	Technical Library	9536 (electronic copy)


Sandia National Laboratories